Cumming, D. A., Shah, R. N., Krepinsky, J. J., Grey, A. A., & Carver, J. P. (1987) *Biochemistry* (first paper of three in this issue).
Dais, P., Shing, T. K. M., & Perlin, A. S. (1984) *J. Am. Chem. Soc. 106*, 3082-3089.
Gueron, M., Chachaty, C., & Son, T.-D. (1973) *Ann. N.Y. Acad. Sci. 222*, 307-323.
Jardetzky, O. (1980) *Biochim. Biophys. Acta 621*, 227-232.
Jardetzky, O., & Roberts, G. C. K. (1981) *NMR in Molecular Biology*, Academic, New York.
Keepers, J. W., & James, T. L. (1982) *J. Am. Chem. Soc. 104*, 929-939.
Kitaigorodsky, A. I. (1961) *Tetrahedron 14*, 230-236.
Kitaigorodsky, A. I. (1978) *Chem. Soc. Rev. 7*, 133-163.
Lemieux, R. U., Bock, K., Delbaere, L. T. J., Koto, S., & Rao, V. S. (1980) *Can. J. Chem. 58*, 631-653.
Mackie, W., Sheldrick, B., Akrigg, D., & Perez, S. (1986) *Int. J. Biol. Macromol. 8*, 43-51.
Marchessault, R. H., & Perez, S. (1979) *Biopolymers 18*, 500-521.
Noggle, J. H., & Schirmer, R. E. (1971) *The Nuclear Overhauser Effect*, Academic, New York.
Perez, S., Taravel, F., & Vergelati, C. (1985) *Nouv. J. Chim. 9*, 561-564.
Potenzone, R., & Hopfinger, A. J. (1975) *Carbohydr. Res. 40*, 322-336.
Ramachandran, G. N., & Sasisekharen, V. (1968) *Adv. Protein Chem. 23*, 283-437.
Rees, D. A., & Scott, W. E. (1971) *J. Chem. Soc. B*, 469-479.
Shah, R. N., Cumming, D. A., Grey, A. A., Carver, J. P., & Krepinsky, J. J. (1986) *Carbohydr. Res. 153*, 155-161.
Thorgersen, H., Lemieux, R. U., Bock, K., & Meyer, B. (1982) *Can. J. Chem. 60*, 44-57.
Tvaroska, I., Perez, S., & Marchessault, R. H. (1978) *Carbohydr. Res. 61*, 97-106.
Venkatachalam, C. M., & Ramachandran, G. N. (1967) in *Conformation of Biopolymers* (Ramachandran, G. N., Ed.) Vol. I, p 83, Academic, New York.
Woessner, D. E., Snowden, B. S., & Meyer, G. H. (1969) *J. Chem. Phys. 59*, 719-721.

Reevaluation of Rotamer Populations for 1,6 Linkages: Reconciliation with Potential Energy Calculations†

Dale A. Cumming and Jeremy P. Carver*
Departments of Medical Genetics and Medical Biophysics, University of Toronto, Toronto, Ontario, Canada M5S 1A8
Received May 28, 1986; Revised Manuscript Received April 3, 1987

ABSTRACT: Applications of ensemble averaging to the solution conformation of model compounds for N-linked glycans are further investigated. Specifically, the interpretation usually applied to observed values of $J_{5,6'}$, a parameter reflecting the rotameric distribution about C5-C6 bonds (torsion angle ω in 1,6 glycosidic linkages) in 6-O-substituted hexopyranosides, was found to be inconsistent with populations derived from potential energy calculations. However, agreement between observed and calculated, ensemble-averaged values of $J_{5,6'}$ was obtained and the distribution of ω rotamers reinterpreted. Values of $J_{5,6'}$ that were previously interpreted as indicative of equipartition between two rotamers in fact reflect a marked preference for one of them. Additional potential energy terms, previously absent from energy calculations, are introduced and shown to be without effect on interpretations of ω rotamer distributions. From comparisons with both NMR relaxation and scalar coupling constant data, it is concluded that a simple empirical algorithm, HSEA, calculating van der Waals, exo-anomeric, and (as appropriate) hydrogen-bonding terms, is best suited for describing the population distributions in solution for oligosaccharides and N-linked glycans.

In the previous paper (Cumming & Carver, 1987), we demonstrated that analysis of the solution conformation of glycans is predicated, first and foremost, upon potential energy calculations, which allow determination of the distribution of conformers about a given linkage in solution. Because they are averages, constraints upon internuclear distances determined by NMR[1] may not realistically reflect those present in solution. Thus, the utility of NMR in such investigations is to confirm calculated population distributions. In this paper, we extend our ensemble calculations to another NMR parameter of principle import to glycan conformational analysis, investigate the effects upon population distributions in conformational space of other interaction terms frequently absent from potential energy algorithms, and illustrate a situation where even ensemble averaging fails to account for the experimentally observed population of conformers in solution.

Experimental Procedures

Computational Procedures. Methods for the calculation of steric interactions and rotational potential energies were presented in the preceding (Cumming & Carver, 1987). Contributions to the potential energy due to the "Hassel-Ottar" (HO) effect (Hassel & Ottar, 1947; Marchessault & Perez, 1979) were also calculated in conjunction with the four potential energy algorithms. The HO contribution, as a

† This research supported by Grants MT-3732 and MA-6499 from the Medical Research Council of Canada.
* Address correspondence to this author.

[1] Abbreviations: HO, Hassel-Ottar effect; Man, D-mannopyranose; GlcNAc, 2-acetamido-2-deoxy-D-glucopyranose; NMR, nuclear magnetic resonance spectroscopy; SDDS, spin-decoupling difference spectroscopy; COSY, homonuclear shift correlated spectroscopy; HSEA, van der Waals + exo-anomeric effect; HSEL, van der Waals + electrostatic; HEAH, van der Waals + exo-anomeric effect + hydrogen bonding; HSEH, van der Waals + electrostatic + hydrogen bonding; PFM, potential function methods; MPL, maximum (normalized) probability of any microstate in an ensemble.

0006-2960/87/0426-6676$01.50/0

function of the glycosidic torsion angle ω, was calculated according to a fitted Gaussian function spanning 120° and centered either at $\omega = +60°$ (for substituted gluco-type residues) or at $\omega = 180°$ (for substituted galacto-type residues). The parameters of the Gaussian were empirically adjusted to fit the shape of the population distribution about ω calculated for 1,6-linked disaccharides.

Values for the vicinal coupling constant $J_{5,6'}$ describing relative populations of rotamers about the C5–C6 bond in hexopyranosides were calculated by two procedures. First, the observed coupling constant was calculated as the sum of the products of the fractional population of each of the ($i = 3$) possible staggered rotamers multiplied by its associated three-bond coupling constant:

$$J_{5,6'} = \sum_i P_i J_i$$

where P_i is the fractional population of the ith rotamer. The second procedure calculates $J_{5,6'}$ as a function of the dihedral angle (θ) in 5-deg increments over the range 30°–330°. The value of $J_{5,6'}$ at each increment was multiplied by a weighting factor corresponding to the fraction of the normalized population found with the corresponding ω value. These weighting factors were derived, as described in the preceding paper, from a Boltzmann distribution based on the three-dimensional potential energy surface calculated for rotation about the 1,6-linkage. Values for the vicinal coupling constant at each increment of the dihedral angle were calculated by utilizing the truncated Taylor-series generalization of the Karplus equation (Haasnoot et al., 1980) as applied to carbohydrates (Altona & Haasnoot, 1980). In this formulation, $J_{5,6'}$ is given by

$$J_{5,6'} = P_1 \cos^2\theta + P_2 \cos\theta + \sum_i \Xi(P_4 + P_5 \cos^2\{\xi_i\theta + P_6\Xi\})$$

where Ξ is the difference in electronegativity (Huggins, 1953) between the substituting atom and hydrogen, and ξ_i the substituent orientation factor, which assumes values of ± 1 (Haasnoot et al., 1980). Values for the parameters P_1–P_6 were obtained for α1,6- and β1,6-substituted Man residues as described elsewhere (Cumming and Carver, manuscript in preparation). All other calculations were performed as described previously (Brisson & Carver, 1983b). All calculations were carried out on a VAX 11/780 located at the Ontario Cancer Institute.

Other Methods. Samples were prepared for, and ^{1}H NMR was carried out, as described previously (Brisson & Carver, 1983a,b; Carver et al., 1987). Details of the chemical synthesis of the model compounds employed herein will be presented elsewhere (Shah et al., 1986; Shah et al., unpublished results).

Results

Potential Energy Calculations and the α1,6 Linkage. Specification of the solution conformers of 1,6 linkages is dependent upon determining the range of possible values assumed for each glycosidic torsion angle. For one of these torsion angles, ω, serious difficulties are often encountered since conformationaly sensitive NOE's and T_1's are often insensitive to variations in ω (Brisson & Carver, 1983a). This is all the more unfortunate in that ω is a primary determinant in the gross orientation of the six-arm in N-linked glycans. Fortunately, an additional spectroscopic parameter is available ($J_{5,6'}$) whose magnitude is directly related to the value(s) of ω (Brisson & Carver, 1983d; Ohrui et al., 1985). Two possible interpretations can be attached to experimentally determined $J_{5,6'}$ values. In the first approach, subpopulations for each of the three possible staggered rotamers are derived. Since only two of the three possible rotamers are thought to exist for any 1,6 linkage (Marchessault & Perez, 1978), the observed $J_{5,6'}$ is taken as the weighted average of the coupling constants for the two staggered rotamers. This approach has previously been employed in estimating the relative abundance of rotamers in synthetic oligosaccharides (Gagnaire et al., 1973; De Bruyn & Anteunis, 1976; Bock et al., 1982; Brisson & Carver, 1983b; Ohrui et al., 1985) and in N-linked glycans (Brisson & Carver, 1983c; Homans et al., 1986). For example, the observed $J_{5,6'}$ of 5.5 Hz for the 6-O-substituted β-linked Man residue in a complex, biantennary glycopeptide was interpreted as reflecting approximately equal populations of the $\omega = 180°$ ($J_{5,6'} = 2$ Hz) and $\omega = -60°$ ($J_{5,6'} = 8$ Hz) rotamers (Brisson & Carver, 1983c). If we term this formulation a "jump-state" model, then the alternative formulation is that a "continuum" of ω values is present. The observed $J_{5,6'}$ may be interpreted not as the weighted average of two or three staggered rotamers but as the weighted average of all possible values of ω, where the weighting factors are derived as the normalized fractional population possessing a given value of ω. In oligosaccharides, a similar approach was employed in evaluating transglycosidic $^3J_{H-C}$ coupling constants by Perez et al. (1985). Support for this alternative interpretation is found in the observation that the rotational potential energy barriers are less than 3 kcal/mol. The distinction between these two approaches is not trivial since significantly different conclusions about the relative populations of rotamers in solution result. In the following, results obtained with each of these formulations will be compared with observed values.

The disaccharide Man(α1,6)Man(β)OMe (compound I) is a simple model compound for the evaluation of ω values in solution. Estimation of $J_{5,6'}$ for the 6-O-substituted β-Man residue in compound I was obtained by spectral analysis of its ^{1}H NMR spectrum. A total spectral analysis was possible through spin-decoupling, SDDS, and COSY analysis and spectral simulation, the results of which are summarized in Table I. As indicated in the Table I, a value of $J_{5,6'}$ of 5.5 Hz for the β-Man residue was observed. As noted above, a jump-state approach (method 1 under Experimental Procedures) shows that this value corresponds to an approximately equal proportion of the two possible rotamers ($\omega = -60°$ and 180°) being present in solution (Brisson & Carver, 1983b,c). Similarly, insertion of the relevant data into the set of simultaneous equations utilized by Ohrui et al. (1985) yields a population distribution enriched in the $\omega = 180°$ rotamer (Table I). However, the question arises as to whether this interpretation of $J_{5,6'}$ agrees with ω rotameric distributions predicted by potential energy calculations.

Other studies have dealt with the potential energy surfaces for 1,6 linkages (Rees & Scott, 1971; Tvaroska et al., 1978). In particular, the latter report investigated the isoenergy maps generated in "conformational space" (whose coordinate axes are defined by the three glycosidic torsional angles which specify the linkage) for α1,6 homopolymers by calculation of potential energy as a function of ϕ and ψ at fixed values of ω. As a result of their study, the major characteristics of α1,6 potential energy surfaces were summarized as follows: (1) The angle ω is the most restricted of the three torsional angles. Potential energy minima are located along the ω axis which correspond to the three rotameric subpopulations about the aglyconic C5–C6 bond. These rotamers and their respective minima are further characterized by angular values spaced 120° apart: –60°, +60°, and 180°. (2) The range of possible values of ϕ is also restricted, though less so than for ω; most

Table I: Summary of Observed Spectral Parameters for Compound I and Related Sugars[a]

compound	chemical shifts						
	H1	H2	H3	H4	H5	H6	H6′
Man(β)OMe	4.575	3.982	3.632	3.560	3.373	3.934	3.733
Man(β) in I	4.581	3.990	3.624	3.669	3.528	3.812	3.951
Man(α) in I	4.917	3.993	3.837	3.660	3.710	3.898	3.758
Man(α)OMe	4.762	3.930	3.756	3.636	3.611	3.899	3.754

compound	coupling constants						
	$J_{1,2}$	$J_{2,3}$	$J_{3,4}$	$J_{4,5}$	$J_{5,6}$	$J_{5,6'}$	$J_{6,6'}$
Man(β)OMe	1.0	3.2	9.8	10.2	2.3	6.7	−12.2
Man(β) in I	1.0	3.4	9.4	9.5	2.0	5.5	−11.2
Man(α) in I	1.7	3.4	9.3	9.7	1.8	6.1	−12.2
Man(α)OMe	1.7	3.5	9.6	9.8	2.0	6.0	−12.3

	C5–C6 rotameric distributions (%) for ω (deg) equal to		
	180	−60	+60
Man(β) in I[b]	50	50	
Man(β) in I[c]	58.1	40.6	1.3
Man(α) in I[b]	50	50	
Man(α) in I[c]	52.7	46.9	0.4

[a] Chemical shifts are given in ppm and referenced to internal acetone at 2.225 ppm (indirectly to sodium 2,2-dimethyl-2-silapentane-5-sulfonate). Nominal probe temperature was 23 °C, and the average error is 0.003 ppm. Coupling constants are given in hertz. Values of chemical shifts and coupling constants for tightly coupled spin systems were estimated by spectral simulation. Chemical shifts and coupling constants for Man(α)OMe and Man(β)OMe are taken from Brisson and Carver (1983a). [b] Population distribution calculated from the coupling constants found for each staggered rotamer according to Brisson and Carver (1983b,c) assuming no ω = +60° rotamer. [c] Population distribution calculated with the set of simultaneous equations of Ohrui et al. (1985).

values fall in the range −60° to 0°. (3) Values of ψ are the least restricted and impart most of the conformational flexibility in solution. Generally, φ, ψ isoenergy contour surfaces obtained at fixed values of ω possess multiple minima aligned along the ψ axis.

Figure 1A illustrates these characteristics for the 1,6 linkage in compound I. The isoenergy contour surface was generated with the HSEA algorithm as a function of φ and ψ while holding ω constant at −60° for the terminal mannose residue and using values of ω for the substituted mannose of −60°. Two local minima are observed although the minimum at ψ = 95° is less than half the depth of the local minimum at ψ = ∼200°. An analogous surface was obtained with the HSEA algorithm if the 6-O-substituted Man ω is fixed at 180°. Several characteristics of these surfaces are listed in Table II. The potential energy surfaces obtained with the HSEA and HEAH algorithms differ in two respects. First, the position and depth of the global minimum in each are different; the ω = −60° surface has a deeper minimum that occurs at the ψ value 20° away from the corresponding minimum in the ω = 180° surface. Second, the total integrated negative potential energy in the two surfaces are different (Table II). These differences correspond (considering only the potential energy at each minimum) to a ratio of ω = −60° to ω = 180° rotamers of 1.9. This ratio is clearly at odds with the calculated populations listed in Table I, which show ratios less than or equal to 1. Two possibilities exist that could explain this inconsistency: either the potential energy algorithms are deficient (such that the calculated energy surfaces cannot give a realistic representation of rotameric distributions), or the interpretation attached to the observed $J_{5,6'}$ is wrong. We will consider each of these possibilities in turn.

In the previous paper, three-dimensional potential energy lattices for the disaccharide Man(α1,6)Man(β)OMe, as a function of the three glycosidic torsion angles defining the α1,6 linkage, were calculated with four different potential energy algorithms (see Figures 1 and 2 in the preceding paper). In contrast to the first characteristic stated above (Tvaroska et al., 1978), this mode of presentation clearly shows that the torsion angle ω is no more restricted than ψ, an attribute contributing to the extensive delocalization in conformational

Table II: Summary of Selected Characteristics of Potential Energy Calculations on Compound I

algorithm	ω (deg)		energy minimum[a]	position (φ, ψ, ω)[b]	integrated neg PE[c]
	Man(β)	Man(α)			
HSEA	−60	−60	−2.23	−48, 210, −60	−997.02
HSEA	−60	180	−2.13	−48, 208, −60	−927.36
HSEA	180	−60	−1.85	−50, 190, 180	−813.96
HSEA	180	180	−1.78	−50, 190, 180	−770.06
HEAH	−60	−60	−2.25	−48, 210, −60	−1017.1
HEAH	−60	180	−2.15	−48, 208, −60	−947.21
HEAH	180	−60	−2.98	−42, 210, 180	−929.56
HEAH	180	180	−1.79	−50, 190, 180	−738.53

[a] Minimum potential energy in kcal/mol. [b] Torsion angle values corresponding to energy minimum, in degrees. [c] Sum of potential energies for all lattice points associated with a minimum. Lattice points were generated, for a fixed value of ω, by calculating the potenial energy as a function of φ and ψ and incrementing φ and ψ in 5-deg steps. Lattice points were associated with a minimum if, when a spiral ascent from the minimum was performed, the first derivative did not change sign (or equal zero) and the potential energy at that lattice point did not exceed −0.5 kcal/mol.

space determined for this linkage in the preceding paper. The second and third characteristics, though, are clearly evident. For each generated lattice, the fraction of the normalized molecular population can be calculated as a function of ω. An example of one distribution is shown in Figure 3 for the lattice calculated with the HSEA algorithm. These ω-dependent distributions can be utilized to calculate a corresponding $J_{5,6'}$ by the two methods described under Experimental Procedures. Table III lists the results of both approaches as applied to compound I. In general, estimation of $J_{5,6'}$ by the first method yields values higher than the observed coupling while the latter procedure gives estimates in good agreement with the observed $J_{5,6'}$. The reason for the difference can be understood if it is realized that the fraction of the molecular population possessing a dihedral angle exactly corresponding to the individual staggered rotamers is quite small and that, given the shape of the modified Karplus curve describing the relationship of the dihedral angle to $J_{5,6'}$, a sizable fraction of the population with ω values near, for example, −60° will exhibit $J_{5,6'}$ values less than the maximum trans coupling associated with ω = −60°. We therefore conclude that it is a rigorous calculation

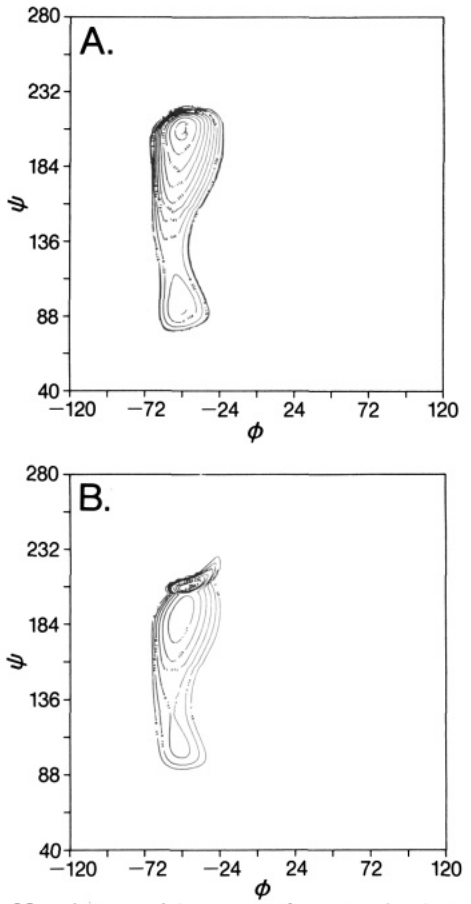

FIGURE 1: Negative potential energy surface maps for the Man(α1,6) linkage in the disaccharide Man(α1,6)Man(β)OMe. Potential energy surface maps, as a function of ϕ and ψ, and at the indicated fixed values of ω, were calculated for rotation about the Man(α1,6) linkage as described under Experimental Procedures. A 120 × 120 array was calculated yielding 2-deg resolution in ϕ and ψ. The 12 contour levels in all the plots are defined as the following percentages of the minimum (most negative) value in the array: 99.0, 95.0, 85.0, 75.0, 65.0, 55.0, 45.0, 35.0, 25.0, 15.0, 5.0, and 3.0. The ω for the terminal Man(α) residue is −60° in both (A) and (B). In the remainder of the legend, ω refers to the torsion angle of the *substituted* Man residue. (A) Isoenergy contour surface generated with the HSEA algorithm at ω = −60°. (B) Contour surface generated with the HEAH algorithm with ω = 180°.

of $\langle J_{5,6'} \rangle$ that yields agreement between experimental data and empirical potential energy algorithms. It is of interest to note that, for $J_{5,6'}$ values previously interpreted as reflecting a 1:1 ratio of rotamers, an ω = −60°/180° ratio approaching 2:1 is obtained from the HSEA and HEAH potential energy algorithms. In the preceding paper, these algorithms were shown to yield the best agreement between other experimentally observed and calculated ensemble averaged NMR relaxation data.

While these results support interpretation of $J_{5,6'}$ values through a "continuum" formulation, they do not unequivocally invalidate an interpretation based upon the jump-state formalism. Deficiencies in the potential energy algorithms may exist such that the $J_{5,6'}$ values calculated by the jump-state approximation are in poor agreement both with the ensemble averaged prediction of rotameric subpopulations (Table II) and with rotameric distributions obtained from potential energy surfaces calculated at fixed values of ω. As mentioned above, these deficiencies could be of several types. Two possible deficiencies will be considered here. The first of these is the omission of intramolecular hydrogen-bonding interactions. For the ω = −60° rotamer, only negligible effects can be found (data not shown). However, for the ω = 180° rotamer (Figure 1B), a substantial (negative) potential energy increment results in a new global minimum of −2.98 kcal/mol at ϕ, ψ = −42°, 210° and an increase in the integrated negative potential energy to levels more comparable to the ω = −60° rotamer (Table II). This additional increment is solely due to hydrogen-bond formation between the C6 hydroxyl of the Man(α1,6) residue and O4 of the β-Man (O···O distance = 2.87 Å at ϕ, ψ = −42°, 210°). However, formation of this hydrogen bond is strongly dependent upon the ω torsional angle for the *Man*(α1,6) residue, which can also freely interconvert between possible ω rotamers (−60 and 180°) (Brisson & Carver, 1983a). This presumption is substantiated by the shift analysis summarized in Table I. The value of $J_{5,6'}$, calculated by spectral simulation (H5 and H6′ are tightly coupled) for the Man(α) residue, is 6.1 Hz (compared to 6.0 Hz in α-MeMan) and is therefore consistent with free interconversion between the two rotamers. When the value of ω for the Man(α) residue is 180°, hydrogen-bond formation is not possible and the generated potential energy surface is analogous to that in Figure 1A. Thus, interconversion of the β-Man C5–C6 rotamer from −60 to 180° should result in, at most, 50% of the molecules forming a hydrogen bond when the ω of the terminal Man(α) residue has values near 180°. The inclusion of a hydrogen-bond interaction is also seen to have only marginal effects in the calculated rotameric subpopulations and $\langle J_{5,6'} \rangle$ obtained from the three-dimensional potential energy arrays (Table III). Therefore, inclusion of a hydrogen-bonding term alone is insufficient to resolve the discrepancy between potential energy calculations and the value of $J_{5,6'}$ predicted by the jump-state model.

An additional interaction absent from these potential energy algorithms is the Hassel–Ottar effect (Hassel & Ottar, 1947). This effect has been invoked to rationalize the absence of one of the three possible rotamers (ω = +60°) in a survey of crystal structures of 1,6-substituted gluco-type oligosaccharides (Marchessault & Perez, 1979). In these oligosaccharides, the energy contribution arising from an unfavorable syn-axial interaction between O4 and O6 of the 6-substituted residue, which occurs in this compound when ω = +60°, has been estimated to be +3.0 kcal/mol (Marchessault & Perez, 1979), although the magnitude of this effect may be partially offset

Table III: Summary of Rotameric Populations and $J_{5,6'}$ Calculated from Various Potential Energy Algorithms[a]

	ω			$J_{5,6'}$	
algorithm	+60°	−60°	180°	method 1[b]	method 2[c]
HSEA	15.2	56.5	28.3	6.4	5.6
HEAH	14.3	53.3	32.4	6.1	5.4
HSEA + HO[d]	1.2	65.8	33.0	6.7	5.8
HEAH + HO[d]	1.2	61.5	37.3	6.3	5.5
HSEL	10.9	52.2	36.9	5.9	5.3
HSEH	11.9	47.4	40.7	6.0	5.1
HSEL + HO[d]	0.7	58.2	41.1	5.6	5.4
HSEH + HO[d]	0.7	53.4	45.9	5.7	5.2

[a] The population associated with each staggered rotamer is defined as the sum of the normalized population that possess ω values ±60° of the specified rotameric ω value. For example, the population of the ω = +60° rotamer consists of that fraction of the normalized population with ω values 0–120°. The procedure for calculating normalized populations from a three-dimensional potential energy surface is detailed in the preceding paper. The experimentally observed value of $J_{5,6'}$ is 5.5 +0.3 Hz. The value of ω for the terminal Man(α) residue was set to −60° for all calculations. [b] Value of $J_{5,6'}$ calculated from the normalized population distribution according to the first method outlined under Experimental Procedures. [c] Value of $J_{5,6'}$ calculated from the normalized population distribution according to the second method outlined under Experimental Procedures. [d] Contributions to the potential energy from the Hassel–Ottar effect have been included as described under Experimental Procedures.

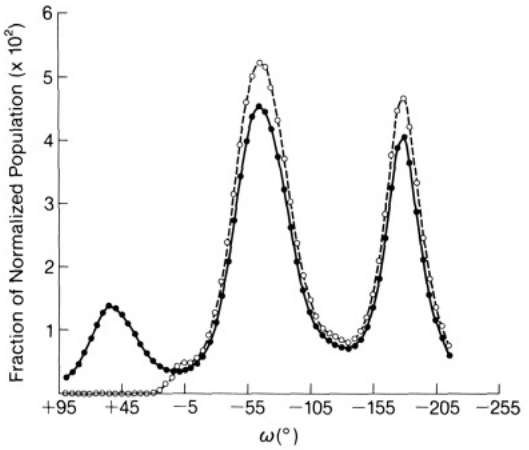

FIGURE 2: Normalized population distribution as a function of ω for the 1,6 linkage in compound I. The normalized distribution in three-dimensional conformational space, for rotation about the α1,6 linkage in Man(α1,6)Man(β)OMe, was calculated as described in the preceding paper. This figure corresponds to the projection of that distribution along the ω axis of conformational space. The HSEA algorithm was used to calculate the potential energy at each lattice point. (●) HSEA; (○) HSEA + HO.

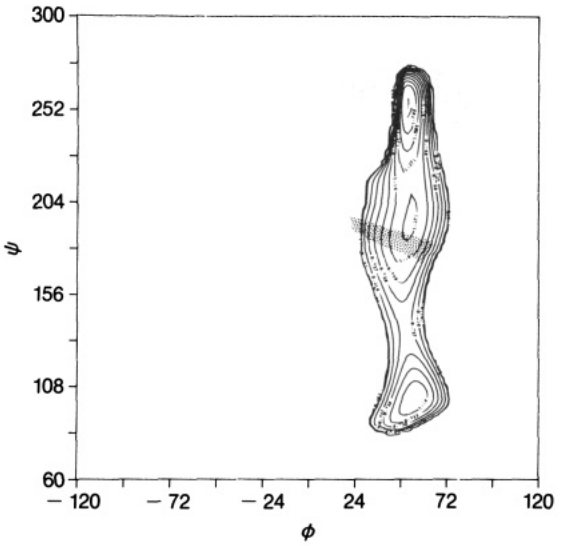

FIGURE 3: Negative potential energy surface map for the GlcNAc-(β1,6) linkage in the trisaccharide GlcNAc(β1,2)[GlcNAc(β1,6)]-Man(α)OMe. Details of the calculation of these contour maps are the same as in the legend to Figure 1 except that the resolution in ϕ and ψ is 3°. The torsion angle ω for this 1,6 linkage is fixed at −60° in accordance with experimental observations. Potential energies were calculated with the HSEA algorithm. Three local minima are observed at ϕ, ψ = 55°, 252° (−4.2 kcal/mol), 55°, 200° (−3.0 kcal/mol), and 55°, 90° (−2.8 kcal/mol). The presence of multiple local minima aligned along the ψ axis is characteristic of a 1,6 linkage. If the potential energy surface is recalculated with the HSEL potential, five local minima are observed at ϕ, ψ = −20°, 88° (−4.7 kcal/mol), 7°, 175° (−5.3 kcal/mol), 30°, 209° (−6.3 kcal/mol), 55°, 260° (−6.0 kcal/mol), and 40°, 88° (−4.7 kcal/mol). Relative to this latter surface, the HSEH potential generates a single new minimum at ϕ, ψ = 66°, 274°.

by formation of an ω-dependent intraresidue hydrogen bond (Pincus et al., 1975). However, we know of no algorithm that explicitly includes this effect. Its omission results in a minor, yet significant, fraction of rotamers with ω near +60° (Figure 2 and Table III in this paper; Figures 1, 2, and 4 in the preceding paper). This is inconsistent with both the crystal structure observations (Marchessault & Perez, 1979) and the results of a study of selectively deuteriated 1,6 disaccharides in solution (Ohrui et al., 1985), neither of which showed any significant occurrence of this rotamer. Therefore, the potential energy distributions were recalculated, explicitly incorporating the Hassel–Ottar effect as described under Experimental Procedures. The results of these calculations are listed in Table III, and an example is shown in Figure 2. Inclusion of this syn-axial interaction results in almost complete elimination of any of the population from the ω = +60° rotamer. The results in Table III also show, however, that inclusion of the Hassel–Ottar effect has little effect on the relative distribution between ω = −60° and ω = 180° rotamers. Therefore, the Hassel–Ottar effect in itself cannot account for the discrepency between the interpretation of the observed $J_{5,6'}$ with the jump-state model and the results of these potential energy calculations. Moreover, those algorithms yielding relative proportions of ω = −60°/180° closest to 1 (HSEL and HSEH) have also been deemed the poorest representation of the oligosaccharide in solution since calculations of averaged, conformationally dependent NMR relaxation data, based on these same algorithms, yield the poorest agreement with observed data (see preceding paper in this series). We conclude that any discrepancy in the rationalization of experimental and calculated data must lie in the interpretation of the observed $J_{5,6'}$ (i.e., the utilization of the jump-state approximation). While inclusion of these two additional interactions should result in a better empirical description of the behavior of the disaccharide in solution, their effects are not manifest in $J_{5,6'}$. The resulting ambiguity (in that no experimental means to rule out the presence of ω = +60° rotamers in solution exist) should be viewed as the result of having a single experimental parameter from which to define ω.

The 1,6 Linkage in GlcNAc(β1,6)[GlcNAc(β1,2)]Man(α)OMe. In the preceding papers (Cumming et al., 1987; Cumming & Carver, 1987), the solution conformation of the 1,6 linkage in GlcNAc(β1,6)[GlcNAc(β1,2)]Man(α)OMe was shown to be specified experimentally by ϕ, ψ, ω = 55°, 190°, −60°, a conformation subsequently stated to be virtual; again the solution conformation is best described by a two-dimensional (ω is fixed) population distribution defined by Ω[HSEA] (data not shown). In this ensemble, the population is such that ϕ is distributed about 55° while ψ is distributed about two local potential energy minima. This can be illustrated, at a fixed value of ω = −60°, as shown in Figure 3, where the isoenergy contour surface generated with the HSEA algorithm is displayed. Three local energy minima are observed at ϕ, ψ = 55°, 90°, 55°, 200°, and 55°, 252°. The intersection surface defining the experimentally determined solution conformation for ϕ and ψ is shown as a shaded region. The surface calculated with the HSEL algorithm (data not shown) displays many more local minima including a new global minimum at ϕ, ψ = 30°, 209°. Inclusion of hydrogen-bond interaction terms in the potential energy calculations (HSEH algorithm) does not significantly alter this energy surface. Neither of these latter two algorithms generates ensemble averaged observables (⟨NOE⟩'s or ⟨T_1⟩'s) completely consistent with experimental NMR relaxation data (data not shown).

On the other hand, a comparable set of isoenergy surfaces can be generated when ω = 180° (data not shown). These surfaces are similar to those calculated with ω = −60° in that multiple minina of comparable depth are observed. In fact, a comparison of the ϕ–ψ potential energy surfaces at these two values of ω shows a deeper local minimum at ω = 180° than at ω = −60°. However, when ω = 180°, fewer lattice points possess negative potential energy, reflecting a reduction in the number of sterically accessible states. Therefore, we have evaluated the observed $J_{5,6'}$ of the 6-O-substituted Man residue (8.8 Hz) in terms of the ensemble distribution of ω rotamers.

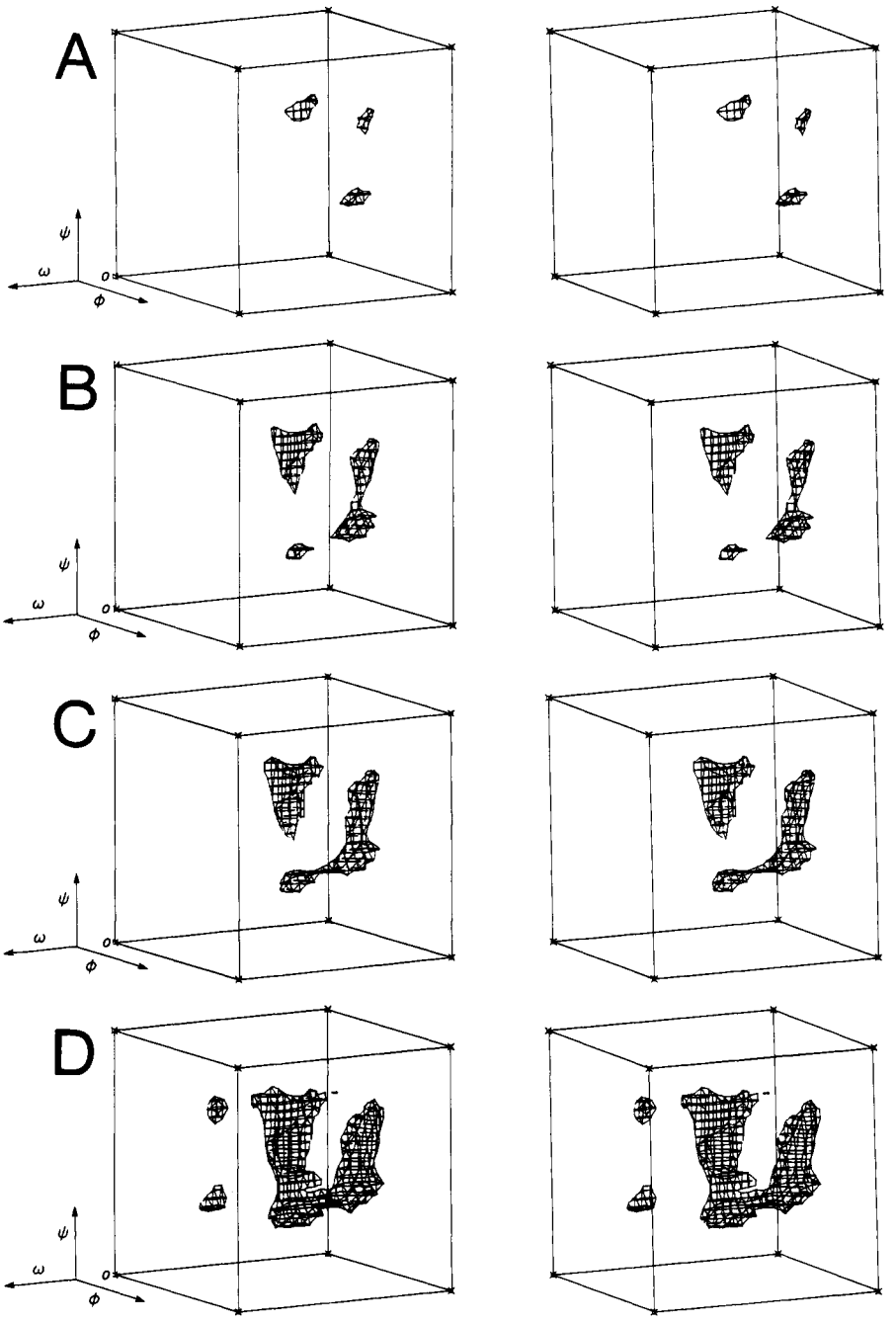

FIGURE 4: Three-dimensional stereo contour surfaces in a calculated ensemble for GlcNAc(β1,6) rotation in GlcNAc(β1,2)[GlcNAc-(β1,6)]Man(α)OMe. Panels A–D show Ω[HSEA] contoured at four "threshold" potential energy values corresponding to 50%, 70%, 80%, and 90% of the normalized population of β1,6-linkage conformers, respectively. As defined in the preceding paper, the threshold potential energy is the value, which upon summing the normalized probability of all microstates possessing a calculated energy equal to or less than the "threshold", yields the specified fraction of the molecular population. The global potential energy minimum for this ensemble of −5.41 kcal/mol is found at ϕ, ψ, ω = 48°, 270°, −102°. The relative origin for each cube is located at the lower left, rear vertex (marked by an o) and corresponds to the point ϕ, ψ, ω = −120°, 0°, 120°. Each axis extends 360° with the positive sense for each labeled axis as marked. The resolution along each coordinate axis is 6° per point.

An ensemble, Ω[HSEA], was calculated as a function of the three torsion angles in the GlcNAc(β1,6) linkage. Analysis of Ω[HSEA] indicates an ω = −60°/180° ratio of ~1.0 and a calculated $J_{5,6'}$ (method 2 under Experimental Procedures) of 5.6 Hz. This is clearly at odds with the experimental value of $J_{5,6'}$, which suggests a population distribution of ω rotamers localized more exclusively about ω = −60°. Panels A–D of Figure 4 show the three-dimensional isoenergy contour surfaces obtained for Ω[HSEA] at threshold potential energy values corresponding to 50%, 70%, 80%, and 90% of the molecular population, respectively. As described in the previous paper, the threshold potential energy corresponds to the minimum volume of conformational space necessary to account for a given percentage of the molecular population. At the 50% level (Figure 4A) discreet volumes are observed, well separated in conformational space, as previously observed in disaccharide 1,6 linkages (preceding paper, Figures 1 and 4). However, in contrast to previously analyzed 1,6 linkages, formation of connectivities along the ω axis does not occur readily. Even at the 90% level (Figure 4D), only a small "tunnel" is observed to connect the two ω subpopulations. This lack of connectivity provides an explanation of the discrepancy between the observed and calculated $J_{5,6'}$ (and hence the distribution among rotameric subpopulations) and points to an inherent limitation

of these potential energy algorithms.

A combination of factors might account for the observed lack of ω interconversion. For example, the potential energy of those microstates that constitute the tunnel along the ω axis is 3–3.5 kcal/mol above the local minima associated with each staggered rotamer. This energy barrier is markedly higher than typically observed in di- and trisaccharides for ω interconversion (1–1.5 kcal/mol). In addition, the tunnel connecting the $\omega = -60°$ and $\omega = 180°$ regions of ϕ, ψ, ω conformational space is confined to a relatively small number of microstates (compare Figure 4D to Figure 2 in the preceding paper). We conclude that the paucity of energetically favorable microstates for ω interconversion will constitute an entropic barrier which, in conjuction with the increased potential energy barrier, provides a possible explanation for the lack of ω interconversion; i.e., the rate of rotamer interconversion is extremely slow due to a free energy barrier that contains a substantial contribution from the unfavorable entropy of activation. Finally, the potential energy algorithm might overlook some stable conformation in the region of $\omega = -60°$. The calculated population distribution in ω would thus be biased with contributions from conformers in the $\omega = 180°$ region. Since the route for chemical synthesis of this trisaccharide presumably specifies a single rotamer, the 1,6 linkage is thereafter "locked" in the potential energy well associated with $\omega = -60°$. Therefore, meaningful population distributions for this linkage in ϕ, ψ, ω conformational space cannot be specified with these potential energy algorithms.

Discussion

Two major conclusions can be drawn from these results. First, the ensemble formulation presented in the previous paper (Cumming & Carver, 1987) can be extended to the interpretation of the scalar coupling constant $J_{5,6'}$, often the only experimentally accessible parameter with which possible values of the torsion angle ω can be evaluated. A reassessment of the interpretation of $J_{5,6'}$ vis-à-vis the distribution of ω rotamers was shown to be necessary. Experimental data that were previously interpreted as specifying equipartition of the population among two rotamers in fact represent a marked preference for one of these ($\omega = -60°$). In combination with the results presented in the preceding paper, it can be seen that the solution conformation for any linkage is represented by the population distribution in conformational space derived from potential energy calculations. While NMR data in itself cannot adequately describe these population distributions, it does provide an invaluable tool for evaluating potential energy algorithms: ensemble averaged relaxation data must agree quantitatively with observed values. Moreover, solution conformations predicated solely upon potential energy calculations are as unacceptable as unaided *quantitative* analysis of NMR data. In particular, assigning a solution conformation on the basis of a global potential energy minimum is clearly misleading and can be erroneous [see the example of the GlcNAc(β1,6) conformation in the trisaccharide GlcNAc-(β1,2)[GlcNAc(β1,6)]Man(α)OMe]. Therefore, solution conformation studies can be defined as the generation of a self-consistent (though not necessarily unique) representation of the molecular population distribution by an iterative refinement of the theoretical model through a comparision with experimental data.

Second, many of the accessory interaction terms utilized in these potential energy algorithms either are experimentally not applicable (e.g., hydrogen-bond interactions) or manifest (e.g., the Hassel–Ottar effect) for any of the disaccharides studied. Only the HSEA algorithm consistently yields population distributions for disaccharides from which calculated, ensemble averaged NMR data (coupling constants, NOE's, and T_1's) are found to be in agreement with observed values. However, it is evident that for larger glycans these accessory terms become more important. For example, even for the GlcNAc(β1,2) linkage in the trisaccharide GlcNAc(β1,2)-[GlcNAc(β1,6)]Man(α)OMe, hydrogen-bond formation is important (see preceding papers in this series). It seems reasonable to anticipate that, in a manner analogous to that observed for proteins and nucleic acids, formation of multiple hydrogen bonds, especially when sterically shielded from the solvent, will become a dominant factor in specifying conformational preferences in larger glycans. Nevertheless, the agreement obtained between experimental and calculated $\langle$NOE$\rangle$'s and $\langle T_1 \rangle$'s from Ω[HSEA] distributions indicates that HSEA is the algorithm of choice for conformational studies of simple oligosaccharides.

The apparent general utility of the HSEA algorithm (Lemieux et al., 1980; Thorgersen et al., 1982) is perhaps somewhat surprising since its applicability, as well as that of empirical algorithms in general, to glycan conformational studies is still the subject of some debate. Potential energy algorithms, such as those employed in this paper, have been termed "potential function methods" (PFM's) (Tvaroska & Bleha, 1985) and are defined as a set of simple, empirical functions employed for complex molecules because of the excessive computational requirements of more reliable quantum mechanical calculations. By definition, PFM's utilize a "classical" potential energy function (in this case van der Waals interactions), which is augmented with additional empirical functions derived (typically) from molecular orbital calculations and represent arbitrary descriptions of the desired effect (in this case, the exo-anomeric effect, electrostatic, Hassel–Ottar, and hydrogen-bonding interactions). Tvaroska and Bleha (1985) have discussed three inherent limitations of PFM's, limitations also observed in these studies: (1) These PFM's either ignore or deal only superficially with solvent effects. Solvent effects have been shown to play a significant role in the conformational equilibria of polar compounds (Tvaroska & Kozar, 1980; Tvaroska & Bleha, 1980; Bleha et al., 1981). Thus, the apparent unsuitability of hydrogen-bonding potential functions in describing conformations of disaccharides may be due to solvent competition and/or entropic effects. In addition, the failure of electrostatic potentials in these studies may be similarly ascribed. These PFM's assume that the oligosaccharide is isolated and in vacuo, thus ignoring the effects of solvent shielding on electrostatic interactions of these neutral, but polar molecules. (2) PFM calculations utilize fixed potential parameters, such as bond lengths and angles, while varying any glycosidic torsion angles despite ample evidence from quantum mechanical calculations that this is not always valid. In the cases reported here, this could be an additional factor with electrostatic potentials (HSEL and HSEH) since the utilized point charges are known to be conformationally sensitive (Pontezone & Hopfinger, 1975). (3) The PFM's are often not of sufficient quality. Because of their semiempirical nature, the augmenting functions often contain contributions from other interactions that may or may not have already been included. There also may be a dependancy on the model compounds used for the quantum mechanical calculations that introduces further bias.

More specifically, the applicability of the HSEA algorithm for calculating conformational energies of oligosaccharides has been questioned recently (Lipkind et al., 1984; Tvaroska & Perez, 1986). In particular, the latter authors conclude, on

the basis of inherent physical inconsistencies and disagreements with experimental data, that the HSEA algorithm (1) overly restricts the calculated flexibility of oligosaccharides and (2) should be avoided for ascertaining the conformational properties of oligosaccharides. On the other hand, recent data from Bock's laboratory (Bock et al., 1985) indicate that the energetic magnitude of the exo-anomeric effect is much larger than 2 kcal/mol, thus further restricting the conformational flexibility of oligosaccharides in solution. Whatever the outcome of these two apparently opposing views, the data presented in these papers clearly indicates the suitability of the HSEA algorithm as originally formulated (Lemieux et al., 1980) for the assessment of the solution conformations of oligosaccharides with ^{1}H NMR data.

Finally, the effects of temperature variation upon ensemble averaging of relaxation data should be mentioned. There are two aspects to this point: the effects of temperature on NMR relaxation rates and upon calculated probability distributions. The temperature dependence of NMR relaxation rates (in the presence of cross-relaxation) is ascribable for dipole–dipole relaxation to the temperature dependence of τ_c (Noggle & Schirmer, 1971). This dependence is functionally exponential in form:

$$\tau_c/\tau_c^0 = \exp(E_a/RT)$$

where E_a is the activation energy (on the order of 4 kcal/mol). Thus, the correlation time is shorter at higher temperatures. The accompanying effect on NOE's or T_1's will depend upon the relative values of $\omega_0\tau_c$; the characteristic dependence of relaxation data upon τ_c is well documented [Kalk & Berendsen, 1976; pp 60 and 64 of Jardetzky and Roberts (1981)]. Observations of invariance for various relaxation data over the temperature ranges typically employed in biological studies have been reported (Kalk & Berendsen, 1976; Noggle & Schirmer, 1971). Similarly, the temperature dependence of ensemble microstate probabilities is also functionally exponential in form. In the high-temperature limit, the probabilities of all ensemble microstates are equalized to $1/N$, where N is the total number of microstates. For temperature variations accessible in aqueous solutions, the effects on probability distributions are much smaller. (This assumes the calculated potential energy of each microstate does not significantly change with temperature. Strictly speaking, this is not true since, for example, the parameterization of nonbonded interactions is dependent upon the magnitude of thermal vibrations.) Our calculations show that increasing the temperature 30 deg results in a 10% decrease in the maximum probability found for any microstate. Thus, significant redistribution of microstate probabilities (and thus significantly altered weighting of microstates) will occur only at much higher temperatures. Therefore, temperature variations of the magnitude encountered in biological studies will generate effects manifested largely in the resulting alteration of τ_c.

ACKNOWLEDGMENTS

We are indebted to Dr. Serge Perez for making the hydrogen-bonding algorithm available to us. We also thank Dr. Brad Bendiak, Dr. Art Grey, Dr. Jim Rini, Marlene Stubbs, and Steven Michnick for critical evaluation of the manuscript and helpful advice.

Registry No. Man(β)OMe, 22277-65-2; Man(α1,6)Man(β)OMe, 100896-85-3; GlcNAc(β1,2)[GlcNAc(β1,6)]Man(α)OMe, 109976-96-7.

REFERENCES

Altona, C., & Haasnoot, C. A. G. (1980) *Org. Magn. Reson. 13*, 417–429.

Bleha, T., Mlynek, J., & Tvaroska, I. (1981) *Collect. Czech. Chem. Commun. 46*, 1722–1733.

Bock, K., Arnarp, J., & Lonngren, J. (1982) *Eur. J. Biochem. 129*, 171–178.

Bock, K., Pedersen, C., Defaye, J., & Gadelle, A. (1985) in *EuroCarbohydrates 1985; Abstracts of the Third European Symposium on Carbohydrates* (Defaye, J., Ed.) p 75, Central University Library Press, Grenoble.

Brisson, J. R., & Carver, J. P. (1983a) *J. Carbohydr. Chem. 2*, 41–55.

Brisson, J. R., & Carver, J. P. (1983b) *Biochemistry 22*, 1362–1368.

Brisson, J. R., & Carver, J. P. (1983c) *Biochemistry 22*, 3680–3686.

Carver, J. P., Cumming, D. A., & Grey, A. A. (1987) in *Glycoprotein Structure and Conformation* (Ivatt, R., Ed.) Plenum, New York (in press).

Cumming, D. A., & Carver, J. P. (1987) *Biochemistry* (second paper of three in this issue).

Cumming, D. A., Shah, R. N., Krepinsky, J. J., Grey, A. A., & Carver J. P. (1987) *Biochemistry* (first paper of three in this issue).

De Bruyn, A., & Anteunis, M. (1976) *Carbohydr. Res. 47*, 311–314.

Gagnaire, D., Horton, D., & Taravel, F. (1973) *Carbohydr. Res. 27*, 363–372.

Haasnoot, C. A. G., DeLeeuw, F. A. A. M., & Altona, C. (1980) *Tetrahedron 36*, 2783–2792.

Hassel, O., & Ottar, B. (1947) *Acta Chem. Scand. 1*, 929–942.

Homans, S. W., Dwek, R. A., Boyd, J., Mahmoudian, M., Richards, W. G., & Rademacher, T. W. (1986) *Biochemistry 25*, 6342–6350.

Huggins, M. L. (1953) *J. Am. Chem. Soc. 75*, 4123–4126.

Jardetzky, O., & Roberts, G. C. K. (1981) *NMR in Molecular Biology*, Academic, New York.

Kalk, A., & Berendsen, H. J. C. (1976) *J. Magn. Reson. 24*, 343–366.

Lemieux, R. U., Bock, K., Delbaere, L. T. J., Koto, S., & Rao, V. S. (1980) *Can. J. Chem. 58*, 631–653.

Lipkind, G. M., Verousky, V. E., & Kochetkov, N. K. (1984) *Carbohydr. Res. 133*, 1–13.

Noggle, J. H., & Schirmer, R. E. (1971) *The Nuclear Overhauser Effect*, Academic, New York.

Ohrui, H., Nishida, Y., Watanabe, M., Hori, H., & Meguro, H. (1985) *Tetrahedron Lett. 26*, 3251–3254.

Perez, S., Taravel, F., & Virgelati, C. (1985) *Nouv. J. Chim. 9*, 561–564.

Pincus, M. R., Burgess, A. W., & Scheraga, H. A. (1975) *Biopolymers 15*, 2485–2521.

Potenzone, R., & Hopfinger, A. J. (1975) *Carbohydr. Res. 40*, 322–336.

Ramachandran, G. N., & Sasisekharen, V. (1986) *Adv. Protein Chem. 23*, 283–437.

Shah, R. N., Cumming, D. A., Grey, A. A., Carver, J. P., & Krepinsky, J. J. (1986) *Carbohydr. Res. 153*, 155–161.

Thorgersen, H., Lemieux, R. U., Bock, K., & Meyer, B. (1982) *Can. J. Chem. 60*, 44–57.

Tvaroska, I., & Bleha, T. (1980) *Collect. Czech. Chem. Commun. 45*, 1883–1895.

Tvaroska, I., & Kozar, T. (1980) *J. Am. Chem. Soc. 102*, 6929–6936.

Tvaroska, I., & Bleha, T. (1985) *Chem. Zvesti. 39*, 805–847.

Tvaroska, I., Perez, S., & Marchessault, R. H. (1978) *Carbohydr. Res. 61*, 97–106.